FINE-SCALE ADAPTATIONS TO ENVIRONMENTAL VARIATION AND GROWTH STRATEGIES DRIVE PHYLLOSPHERE *METHYLOBACTERIUM* DIVERSITY.

Jean-Baptiste Leducq[1,2,3], Émilie Seyer-Lamontagne[1], Domitille Condrain-Morel[2], Geneviève Bourret[2], David Sneddon[3], James A. Foster[3], Christopher J. Marx[3], Jack M. Sullivan[3], B. Jesse Shapiro[1,4] & Steven W. Kembel[2]

1 - Université de Montréal
2 - Université du Québec à Montréal
3 – University of Idaho
4 – McGill University

Key words: *Methylobacterium* diversity, Phyllosphere community dynamics, *rpoB* barcoding, temperature adaptation, growth strategies in *Bacteria*

Abstract

Methylobacterium is a prevalent bacterial genus of the phyllosphere. Despite its ubiquity, little is known about the extent to which its diversity reflects neutral processes like migration and drift, or environmental filtering of life history strategies and adaptations. In two temperate forests, we investigated how phylogenetic diversity within *Methylobacterium* was structured by biogeography, seasonality, and growth strategies. Using deep, culture-independent barcoded marker gene sequencing coupled with culture-based approaches, we uncovered a previously underestimated diversity of *Methylobacterium* in the phyllosphere. We cultured very different subsets of *Methylobacterium* lineages depending upon the temperature of isolation and growth (20 °C or 30 °C), suggesting long-term adaptation to temperature. To a lesser extent than temperature adaptation, *Methylobacterium* diversity was also structured across large (>100km; between forests) and small geographical scales (<1.2km within forests), among host tree species, and was dynamic over seasons. By measuring growth of 79 isolates at different temperature treatments, we observed contrasting growth performances, with strong lineage- and season-dependent variations in growth strategies. Finally, we documented a progressive replacement of lineages with a high-yield growth strategy typical of cooperative, structured communities, in

favor of those characterized by rapid growth, resulting in convergence and homogenization of community structure at the end of the growing season. Together our results show how *Methylobacterium* is phylogenetically structured into lineages with distinct growth strategies, which helps explain their differential abundance across regions, host tree species, and time. This works paves the way for further investigation of adaptive strategies and traits within a ubiquitous phyllosphere genus.

Abstract importance

Methylobacterium is a bacterial group tied to plants. Despite its ubiquity and importance to their hosts, little is known about the processes driving *Methylobacterium* community dynamics. By combining traditional culture-dependent and –independent (metagenomics) approaches, we monitored *Methylobacterium* diversity in two temperate forests over a growing season. On the surface of tree leaves, we discovered remarkably diverse and dynamic *Methylobacterium* communities over short temporal (from June to October) and spatial scales (within 1.2 km). Because we cultured very different subsets of *Methylobacterium* diversity depending on the temperature of incubation, we suspected that these dynamics partly reflected climatic adaptation. By culturing strains in lab conditions mimicking seasonal variations, we found that diversity and environmental variations were indeed good predictors of *Methylobacterium* growth performances. Our findings suggest that *Methylobacterium* community dynamics at the surface of tree leaves results from the succession of strains with contrasted growth strategies in response to environmental variations.

Acknowledgments: FRQNT (funding), NSERC (funding), Canada Research Chairs (funding), NSF (DEB-1831838), Geneviève Lajoie, Dominique Tardif, Ariane Lafrenière, Hélène Dion-Phénix, Yves Terrat, Kenta Araya (help for sampling), Sylvain Dallaire (help for phenotyping screen), Sergey Stolyar (discussions), Gault Natural Reserve (McGill University), Station Biologique des Laurentides (UdeM), Centre d'Étude de la Forêt (CEF), QCBS.

Author contributions : J.B.L., E.S.L., D.C.M., G.B., B.J.S. and S.W.K. planned fieldwork and the experiments. J.B.L. E.S.L., D.C.M. and G.B. performed experiments. J.B.L., E.S.L., D.S. and J.M.S performed bioinformatic analyses. J.A.F., C.J.M. and J.M.S. provided discussion in the

63 early stages of this study. J.B.L. B.J.S. and S.W.K. drafted the manuscript with contributions
64 from C.J.M.
65
66 **Data accessibility:** raw reads for *16s* and *rpoB* barcoding on phyllosphere communities
67 (BioProject PRJNA729807; BioSamples SAMN19164946-SAMN19165146) were deposited in
68 NCBI under SRA Accession Numbers SRR14532212-SRR14532451. Partial nucleotide
69 sequences from marker genes obtained by SANGER sequencing on *Methylobacterium* isolates
70 (BioProject PRJNA730554 ; Biosamples SAMN19190155-SAMN19190401) were deposited in
71 NCBI under GenBank Accession Numbers MZ268514-MZ268593 (*16s*), MZ330152-MZ330358
72 (*rpoB*) and MZ330130-MZ330151 (*sucA*). R codes and related data were deposited on Github
73 (https://github.com/JBLED/methylo-phyllo-diversity).
74
75

Introduction

Phyllosphere, the aerial parts of plants including leaves, is a microbial habitat estimated as vaste as twice the surface of the earth (1). Although exposed to harsh conditions, like UVs, temperature variations and poor nutrient availability, the phyllosphere arbors a diverse community of microorganisms, of which bacteria are the most abundant (1). A key challenge in microbial ecology and evolution is understanding the evolutionary and ecological processes that maintain diversity in habitats such as the phyllosphere. Bacteria living in the phyllosphere carry out key functions including nitrogen fixation, growth stimulation and protection against pathogens (1–3). At broad spatial and temporal scales, bacterial diversity in the phyllosphere varies as a function of biogeography and host plant species, potentially due to restricted migration and local adaptation to the biotic and abiotic environment (4–6), leading to patterns of cophylogenetic evolutionary association between phyllosphere bacteria and their host plants (7). Whether those eco-evolutionary processes are important at short time scales, as microbes and their host plants migrate and adapt to changing climates, is still an open question (8). Another challenge is to link seasonal variation with plant-associated microbial community dynamics, as shifts in microbial community composition are tighly linked with host plant carbon cycling (9) and ecosystem functions including nitrogen fixation (10). More generally, we understand very little about how the ecological strategies of phyllosphere bacteria vary among lineages and in response to variation in environmental conditions throughout the growing season (9, 11).

Phylogenetic signal in traits or suites of correlated traits that are used as indicators of the ecological life history strategy of microbes suggest niche adaptation (12), and these phenotypic traits influence the assembly of ecological communities through their mediation of organismal interactions with the abiotic and biotic environment (13). Recent work evaluating the phylogenetic depth of microbial trait evolution has shown that many microbial phenotype traits exhibit phylogenetic signal, with closely related lineages possessing similar phenotypic traits, although the phylogenetic depth at which this signal is evident differs among traits (14). Most comparative studies of microbial trait evolution have focused on broad scale patterns across major phyla and classes (14), although some studies have found evidence for complex patterns of phenotypic and genomic evolution within microbial genera interacting to determine patterns of

community assembly and niche evolution (15, 16). Furthermore, to date the majority of studies of the diversity of plant-associated microbes have been based on the use of universal marker genes such as the bacterial 16S rRNA gene, providing a global picture of long-term bacterial adaptation to different biomes and host plants at broad phylogenetic scales (17), but lacking sufficient resolution to assess the evolutionary processes at finer spatial and temporal scales that lead to the origin of and adaptations within microbial genera and species (18, 19).

The Rhizobiales genus *Methylobacterium* (*Alphaproteobacteria*, *Rhizobiales*, *Methylobacteriaceae*) is one of the most prevalent bacterial genera of the phyllosphere, present on nearly every plant (20, 21). Characterized by pink colonies due to carotenoid production, *Methylobacterium* are facultative methylotrophs, able to use one-carbon compounds, such as methanol excreted by plants, as sole carbon sources (21–23). Experimental studies have shown the important roles of *Methylobacterium* in plant physiology, including growth stimulation through hormone secretion (24–26), heavy metal sequestration (26), anti-phytopathogenic compound secretion, and nitrogen fixation in plant nodules (27), sparking increasing interest in the use of *Methylobacterium* in plant biotechnology applications (26, 28, 29). Although up to 64 *Methylobacterium* species have been described (30–38), genomic and phenotypic information was until recently limited to a small number of model species: *M. extorquens*, *M. populi*, *M. nodulans*, *M. aquaticum* and *M radiotolerans*, mostly isolated from anthropogenic environments, and only rarely from plants (39–43). Newly available genomic and metagenomic data now allow a better understanding of *Methylobacterium* diversity across biomes (30), but we still understand relatively little about the drivers of the evolution and adaptation of *Methylobacterium* in natural habitats.

In this study, we assessed the diversity of *Methylobacterium* in temperate forests and asked whether *Methylobacterium* associated with tree leaves act as an unstructured population with large effective size, or if this diversity was maintained by regional factors (*e.g.* a combination of isolation by distance and regional environmental variation) or by niche adaptation (*e.g.* host tree or temperature adaptation) (12). First, we assessed *Methylobacterium* diversity by combining culturing and barcoding approaches along with phylogenetic analysis and quantified how this diversity varied across space, time, and environment in the phyllosphere. Second, we quantified

the extent of phylogenetic niche differentiation within the bacterial genus *Methylobacterium*, with a focus on quantifying the evidence for adaptation to local environmental variation at different spatial, temporal and phylogenetic scales. We hypothesized that distinct phylogenetic lineages would be associated with distinct environmental niches. Third, we quantified *Methylobacterium* growth performance under fine-scale environmental variations, with a focus on temperature, to determine whether *Methylobacterium* diversity fine-scale dynamics over space and time might result from environmental filtering of isolates with contrasting growth strategies under local environmental conditions. We found that *Methylobacterium* phyllosphere diversity consisted of deeply branching phylogenetic lineages associated with distinct growth phenotypes, isolation temperatures, and large-scale spatial effects (forest of origin), while finer-scale spatial effects, host tree species, and time of sampling were more weakly and shallowly phylogenetically structured. Over the course of a year, from spring to fall, we observed a homogenization of *Methylobacterium* community structure coinciding with the progressive replacement of isolates with high yield strategy by isolates with rapid growth. Together our results show that this ubiquitous phyllosphere genus is structured into lineages with distinct growth strategies, which helps explain their differential abundance across space and time.

Results

Phylogenetics of plant-associated Methylobacterium diversity.

We evaluated the known *Methylobacterium* diversity associated with plants, especially the phyllosphere, by compiling information about the origin of 153 *Methylobacterium* isolates for which genomes were available. We found that plants (65% of genomes) and especially the phyllosphere compartment (41% of genomes) were the most prevalent source of *Methylobacterium.* From these genomes, we built a phylogenetic tree based on the complete nucleotide sequence of *rpoB*, a highly polymorphic marker that experienced no copy number variation in many bacteria taxa (44, 45), and that we confirmed to be single copy in *Methylobacterium* and related genera *Microvirga* and *Enterovirga* (**Figure 1, Supplementary dataset 1a**). In this phylogeny, we roughly identified main *Methylobacterium* groups (A, B, and C) previously defined based on the 16S gene (30) and found that phyllosphere-associated

diversity was not randomly distributed in the *Methylobacterium* phylogenetic tree. Isolates from the phyllosphere represented the largest part of diversity within group A (56% of isolates) but not in groups B and C (17 and 12% of isolates, respectively). Most of diversity within group A consisted of undescribed taxa falling outside previously well-described linages (**Figure 1, Supplementary dataset 1a**). For the purpose of this study, we refined *Methylobacterium* group A that we subdivided into 9 monophyletic clades (A1-A9), using a ~92% pairwise similarity (PS) cut-off on the *rpoB* complete sequence.

16S Community analyses reveal Methylobacterium ubiquity and diversity in the phyllosphere.

We focused on *Methylobacterium* phyllosphere diversity variation observable at the scale of seasonal variation on individual trees within a geographic region, the temperate forests of northeastern North America (**Figure 2a,b**). In two forests: Mont Saint Hilaire (MSH**;** 45.54 N 73.16 W ; **Figure 2c**) and Station biologique des Laurentides (SBL**;** 45.99 N 73.99 W ; **Figure 2d**), we marked 40 trees representative of diversity observed in 4-6 plots distributed along a 1.2 km transect (4-10 trees per plot). In MSH, the transect followed an elevation and floristic gradient, while in SBL, it followed a relatively constant environment. For this time series, each tree was sampled 3-4 times from June to October 2018 (**Figure 2b; Supplementary dataset 1b**). We evaluated the microbial phyllosphere diversity in our time series based on sequencing and identification of bacterial 16S gene amplicon sequence variants (ASVs; (46)) in a representative subset of 46 phyllosphere samples from 13 trees (**Supplementary dataset 1c-e**). As observed in previous studies (4), the distribution of the phyllosphere bacterial community was mostly explained by differences among forests (31.6% of variation explained; $p<0.001$; PERMANOVA; Hellinger transformation; 10,000 permutations), host tree species (15.6% of variation; $p<0.001$) and time of sampling (12.0%; $p<0.05$; **Table 1**), indicating that between-forest variation and adaptation to hosts were the main drivers of this diversity, which also varied greatly at the time scale of a year. Although representing only 1.3% (0.0-3.2% per sample) of total 16S sequence diversity, *Methylobacterium* was present in almost all analyzed samples (45 out of 46; **Supplementary dataset 1d,e**). We assigned the 15 *Methylobacterium* ASVs identified by 16S sequencing to clades from *Methylobacterium* group A: A9 (*M. phyllosphaerae/M. mesophilicum/M. phyllostachyos/ M. pseudosasicola/M. organophilum;* 0.87% of total diversity,

nine ASVs), A6 (*M. sp.*, 0.29%; one ASV) and A1 (*M. gossipicola*; 0.13%, 3 ASVs; **Supplementary dataset 1e**). With two rare ASVs (<0.01% of relative abundance) assigned to *M. komagatae*, belonging to group A (30) but unrelated to any aforementioned clade, we defined a new clade (A10). No ASV was assigned to group B or group C, hence confirming observations from available genomes that *Methylobacterium* group A is tightly associated with the phyllosphere.

Development of a single-copy molecular marker to monitor fine-scale dynamics of Methylobacterium populations.

Although the 16S barcoding approach suggests that *Methylobacterium* is ubiquitous in the phyllosphere of temperate forests, regardless of location, time and host tree species, identification based on 16S sequencing presents some limits in assessing microbial population dynamics at local scales, and in assessing fine-scale evolutionary adaptations (18). First, the low polymorphism of the 16S rRNA gene does not permit distinguishing among species within clades typical of the phyllosphere, thus confounding species with potentially divergent evolutionary routes reflecting the distinct ecological niches they occupy within the phyllosphere. Second, 16S copy number variation within *Methylobacterium* (4-12) and even within groups of closely related isolates (4-6 copies in group A; 5 in group B; 6-12 copies in group C), may induce biases in estimating relative abundances of taxa, and thus in assessing the dynamics of populations over space, time and among host tree species.

To assess *Methylobacterium* diversity at a finer evolutionary level, we thus developed a molecular marker targeting all members of the *Methylobacteriaceae* family, using the core gene *rpoB* (**Figure 1** (44, 45)). Based upon *rpoB* sequences available for *Methylobacterium* (**Supplementary dataset 1a)**, as well as sequencing of *rpoB* partial sequences from 20 *Methylobacterium* isolates from a pilot survey in MSH in 2017 (**Figure 2d; Table S1; Supplementary dataset 1f,g**) we determined that this gene is polymorphic enough to explore diversity within the aforementioned *Methylobacterium* clades (See **supplementary method**). For the rest of this study, we used the *rpoB* marker to monitor temporal trends in *Methylobacterium* diversity in the phyllosphere from our 2018 time series in both forests.

231

232 *Culture-based assessment of Methylobacterium diversity in the tree phyllosphere.*

233

234 We evaluated the culturable part of *Methylobacterium* diversity from a subsample of 36 trees (18
235 per forest) representative of floral diversity in the 2018 time series in MSH and SBL. To date,
236 *Methylobacterium* was mostly isolated assuming its optimal growth was in the range 25-30 °C
237 (47), an approach that could lead to a bias toward mesophylic isolates in estimating microbial
238 diversity, especially in the case of microbes inhabiting temperate forests where temperatures
239 typically range from 10 to 20 °C during the growing season (48). We thus performed replicate
240 isolation of *Methylobacterium* at both 20 and 30 °C on minimum mineral salt (MMS) media with
241 0.1% methanol as sole carbon source. We successfully amplified the *rpoB* marker for 167 pink
242 isolates that we assigned to *Methylobacterium* based upon their phylogenetic placement
243 (**Supplementary dataset 1g,h; Supplementary method)**. As observed for 16S ASVs, most
244 isolates were assigned to clades from group A typical of the phyllosphere: A9 (59.9% of isolates),
245 A6 (24.6%), A1 (5.4%), A10 (3.6%) and A2 (1.8%). Few isolates were assigned to group B
246 (4.2% of isolates), mostly related to *M. extorquens*, and none to group C (**Table S2**). But the
247 higher polymorphism in the *rpoB* marker allowed us to uncover a considerable diversity within
248 clades, as we identified 71 unique *rpoB* sequences, in contrast to the smaller number obtained
249 with 16S barcoding (15 ASVs).

250

251 Such high diversity in *rpoB* suggests that standing genetic variation is segregating within
252 *Methylobacterium* populations inhabiting the phyllosphere. We hypothesized that the
253 maintenance of this divestity could be explained by regional factors (*e.g.* a combination of
254 isolation by distance and regional environmental variation) and/or by niche adaptation (*e.g.* host
255 tree or temperature adaptation)(12). To do so, we quantified associations between
256 *Methylobacterium* diversity assessed at varying depths in the *rpoB* phylogeny (**Supplementary**
257 **method**; **Figure 3a**) with four factors and their interactions (PERMANOVA with 10,000
258 permutations): (1) forest of sampling (2) temperature of isolation, (3) sampling time, and (4) host
259 tree species. For every phylogenetic depth tested, diversity had distinct associations with forest of
260 origin (4.5±1.0% of variance explained; p<0.001) and temperature of isolation (5.9±2.1% of
261 variance explained; p<0.001; **Figure 3a; Supplementary dataset 1i**). Interestingly, temperature

of isolation was the most important factor distinguishing deep phylogenetic divergences (pairwise nucleotide similarity range: 0.948-0.993), while forest of origin was slightly more important in structuring more recently diverged nodes (pairwise nucleotide similarity >0.993). This suggests that mechanisms underlying isolation success at different temperatures played a significant role in the early divergence among *Methylobacterium* clades associated with tree leaves, while spatial variation among different forests evolved more recently. Time of sampling had a slight but significant effect on diversity (2.1±0.2% of variance explained; $p<0.05$) and it was only observed for higher pairwise nucleotide similarity values (range 0.994-1.000), suggesting seasonal *Methylobacterium* diversity dynamics at the tip of the tree. We did not observe any significant effect of host tree species on *Methylobacterium* isolate diversity, for any level of the phylogeny, suggesting no strong specific associations between *Methylobacterium* isolates and the tree species from which they were isolated.

We next asked specifically which nodes within the *Methylobacterium* phylogenetic tree were associated with the two major factors contributing to overall diversity, namely forest and temperature of isolation (**Figure 3a**). For every level in the *rpoB* phylogeny, we independently tested for nodes (with at least 30% of support) associated with forest of origin (SBL and MSH) or temperature of isolation (20 and 30 °C) by permutation (100,000 permutations per level and per factor; **Figure 3b**). We identified two nodes strongly associated with temperature of isolation and corresponding to clades A6 (20 °C; $p<0.001$) and A9+A10 (30 °C; $p<0.001$; **Figure 3b**). Other clades were evenly isolated at 20 and 30 °C and we observed no significant association between temperature of isolation and nodes embedded within clades. Nodes associated with forest of origin also roughly corresponded to certain major clades, with clades A1+A2 almost exclusively sampled in MSH ($p<0.01$). Overall, clade A9 was isolated significantly more often in SBL ($p<0.001$) but at least three of its subclades were significantly associated to either MSH or SBL ($p<0.05$), suggesting relatively recent migration events. The fact that *Methylobacterium* diversity typical of the phyllosphere show contrasted associations with forest and temperature of isolation suggests that their evolution was tightly linked with processes related to spatial and environmental variation including isolation by distance as well as niche-based processes including adaptation to local climatic conditions.

Comparison of Methylobacterium diversity assessed by rpoB barcoding and isolation

To determine if these culture-based results were representative of the potentially uncultured *Methylobacterium* diversity, we developed a culture-independent barcoded amplicon sequencing approach based on *rpoB.* We performed *rpoB* amplicon sequencing for 179 leaf samples from 53 trees in both forests, allowed a monthly monitoring for most trees (**Supplementary dataset 1c,j**). We identified 283 *Methylobacteriaceae rpoB* ASVs in these samples (**Supplementary dataset 1j,k**), representing 24.6% of all sequences. Non-*Methylobacteriaceae* ASVs were mostly assigned to other Rhizobiales families (850 ASVs, 70.33% of sequence abundance) and to Caulobacterales (209 ASVs, 4.42% of sequence abundance) typical of the phyllosphere (see **Supplementary method**), suggesting that our *rpoB* marker is not limited to *Methylobacteriaceae* and can potentially be used at a broader taxonomic scale (**Figure S1a**). Within *Methylobacteriaceae*, ASVs were mostly classified as *Methylobacterium* (200 ASVs, 23.05% of sequence relative abundance), and *Enterovirga* (78 ASVs, 1.56%; **Supplementary dataset 1k**). We assigned *Methylobacterium* ASVs to previously defined clades using a maximum likelihood tree combining ASV sequences and reference genomes (**Figure S1b**). Most of *Methylobacterium* diversity was within the previously cultured clades A9 (45.2% of *Methylobacterium* sequence abundance), A6 (24.3%), A1 (6.1%) and A10 (1.0%; **Supplementary dataset 1j; Table S2**). Estimates of *Methylobacterium* diversity based on *rpoB* sequences from culture-independent sequencing or cultured isolates were generally concordant (**Figures S1c,d; Table S2**). Nevertheless, we cannot exclude the possibility that some diversity was not isolated. For instance, although 19.1% of total *Methylobacterium* diversity assessed by *rpoB* culture-free barcoding was assigned to group B, it only represented 4.2% of isolates. One possible explanation could be adaptation of some isolates from this group to temperatures below the range used for isolation (20-30 °C), as temperatures at the very beginning (May) and end (October) of the growing period in Quebec typically range between 5 and 15°C.

Fine-scale temporal and spatial distribution of Methylobacterium diversity assessed by rpoB barcoding

Our isolate-based survey suggested that the distribution of *Methylobacterium* diversity was driven by both spatial and seasonal variation. This result was largely supported using the culture-free approach (*rpoB* barcoding). Specifically, we found that spatial variation at both large (distance between forests: 100km) and local scales (distance between plots within forest: 150-1,200 m), as well as sampling date during the growing season (1-5 months), explained the largest part of variance in the community composition of 200 *Methylobacterium* ASVs (proportion of variation explained: 32.4%, 8.0% and 4.8%, respectively; $p<0.001$; PERMANOVA; Hellinger transformation, Bray-Curtis dissimilarity, 10,000 permutations; **Table 1**). A large proportion of *Methylobacterium* ASVs (83 out of 200) were significantly associated with one or either forest (ANOVA; Bonferroni correction; **Figure 4a; Supplementary dataset 1l**), regardless their clade membership. The only exception was observed for clade A1, which was almost exclusively observed (and isolated; see **Figure 3b**) in the MSH forest. Also consistent without our isolation-based results, we found no clear association between ASV or clade with host tree species, nor plots within forests (data not shown).

To focus on temporal variation and fine-scale spatial effects, we removed large-scale spatial variation by analyzing each forest separately. We quantified fine-scale spatial and temporal dynamics of *Methylobacterium* diversity (200 ASVs), using autocorrelation analysis based on Bray-Curtis dissimilarity index (*BC*). We observed a weak but significant decrease of community similarity with geographical distance separating two samples within MSH (ANOVA on linear model; $p<0.001$) but not SBL ($p>0.05$, **Table 2, Figure 4b**), and a significant decrease of community similarity with time separating two samples in both forests (ANOVA on linear model; $p<0.001$; **Table 2**), which was more marked in MSH than in SBL (**Figure 4c**). Both results indicate that *Methylobacteriaceae* diversity is heterogeneously distributed even at very local space and time scales. The overall community dissimilarity consistently decreased from June to October in both MSH (from 0.624 to 0.297) and SBL (from 0.687 to 0.522; **Table 2, Figure 4d**), suggesting that *Methylobacteriaceae* diversity was progressively homogenized by migration or ecological filtering between the beginning and the end of the growing season at the scale of a forest, although without affecting locally its heterogeneous spatial distribution in MSH (**Table 2, Figure 4e**). The heterogeneous spatial distribution of *Methylobacterium* diversity observed in MSH forest suggests either more restricted migration than in SBL, and/or local

adaptation due to environmental gradients. One possible explanation is that the floristic and altitudinal gradient observed in MSH (**Figure 2d**) – but not in SBL – might generate local adaptation to host tree species for *Methylobacterium* colonizing leaves in this more heterogeneous forest, hence counteracting the homogenizing effect of neutral processes like migration (49). Accordingly, we found slight but significant effects of host tree species, and of the interaction between host tree species and plots within forests, on *Methylobacterium* community composition (explaining 7.1% and 4.3% of variation in community composition; $p<0.001$ and ,$p<0.01$, respectively; PERMANOVA; **Table 1**).

We tested for temporal autocorrelation in each node of the ML tree (**Figure S1b**) supported by at least 30% of bootstrapps (200 permutations) and observed significant temporal dynamics (as attested by the positive slope between pairwise time and BC dissimilarity) in most testable nodes (ANOVA, Bonferroni correction; **Figure 4f**). We observed the strongest temporal signals in nodes embedded within clades A1 (MSH) and B (both forests), Accordingly, we found 25 ASVs whose abundance significantly increased thourough the growing season (ANOVA; Bonferroni correction; $p<0.05$), mostly belonging to clades A1 (n=11). Four ASVs increased significantly with time in both forests and mostly belonged to group B (n=3), suggesting that at least a part of the characteristics driving short-term dynamics of *Methylobacterium* communities are shared among members of different clades within the genus (**Supplementary dataset 1l**).

Effect of short scale temperature variation in combination with other environmental and genetic factors on Methylobacterium growth performances

A major environmental difference between forest sites and throughout the growing season relates to shifts in temperature, suggesting, together with temperature preference of some clades during the isolation step, that *Methylobacterium* diversity dynamics we observed over space and time might result from clade contrasted growth performances under local climatic conditions. To further explore the role of temperature, we measured growth of 79 *Methylobacterium* isolates (sampled in 2018 in both forests; MSH: n=32, SBL: n=47 ; **Supplementary dataset 1m**) for four temperature treatments mimicking temperature variations during the growing season. Each treatment consisted of an initial pre-conditioning step (*P*) during which each isolate was

incubated on solid MMS media with methanol as sole carbon source for 20 days at either 20 °C (*P20*) or 30 °C (*P30*), and a second monitoring step (*M*) during which pre-conditioned isolates were incubated on the same media and their growth monitored for 24 days at 20 °C (*P20M20* and *P20M30*) or 30 °C (*P30M20* and *P30M30*; **Figure S2**). Treatments *P20M20* and *P30M30* mimicked stable thermal environments, and treatments *P20M30* and *P30M20* mimicked variable thermal environments. For each isolate and temperature treatment, logistic growth curves were inferred from bacteria spot intensity variation observed over three time points during the monitoring step (**Figures S2, S3**). From growth curves, we estimated maximum growth intensity, or yield (*Y*) and growth rate (*r*) as the inverse of lag+log time necessary to reach *Y* (**Figure S4** (50, 51)). Clade membership explained a large part of variation in *Y* and *r* (30.6 and 7.6% of variation explained, respectively; ANOVA; $p<0.001$), indicating that *Methylobacterium* growth performance is largely long-term inherited and tends to be shared among clade members (**Figures 5a,b, Table 3**). Certain clades had a higher yield range than others, suggesting differences in their carbon use efficiency (51), here provided by methanol. For example, group B isolates ($Y = 12.2 \pm 5.0$) have higher yield than group A ($Y = 5.4 \pm 3.5$). Different growth rates rather suggest contrasted growth strategies across clades (51, 52). Isolates from clades A1, A2 and B had the highest growth rate (*r* range: 0.101±0.032 – 0.121±0.031), suggesting they have fast-growth strategy. Other clades (A6, A9 and A10) had on average slower growth (*r* range: 0.082±0.021 – 0.088±0.024), suggesting that they have more efficient strategy (51).

Compared to clade membership, we observed that time of sampling, host tree species and forest explained less variation in growth rate (5.4%, $p<0.001$; 2.2%, $p<0.01$ and 1.5%, $p<0.05$, respectively; ANOVA; **Table 3**), suggesting that plasticity to the environment was a secondary but still determining factor in strain growth strategy. The weak or non-significant interactions between clade membership and the aforementioned environmental factors (ANOVA; **Table 3**) suggest that these patterns were consistent across clades, indicating they are unlikely to result from long-term adaptation but rather correspond to short-term responses to environmental conditions. In both SBL and MSH, growth rate increased consistently from June (r = 0.075±0.018 and 0.085±0.033, respectively) to September/October (r = 0.097±0.031 and 0.103±0.027, respectively; **Figure 5c**). Growth rate increase thorough the season might result from increasing competition within phyllosphere communities, for instance by selection for faster

416 growth. Accordingly, culture-independent *rpoB* confirmed that clades associated with faster
417 growth (clades B and A1) increased in abundance over time.
418
419 Temperature also had significant effects on growth performance. Temperature during the
420 monitoring phase explained respectively 2.0% and 15.8% of variation in yield and growth rate
421 (p<0.01 and p<0.001, respectively; ANOVA; **Figure 5d, Table 3**), regardless of clade
422 membership (no significant interaction in the ANOVA). Isolates incubated at 20 °C have on
423 average higher yield (Y=6.9±5.4) but slower growth (r=0.077±0.022) than isolates incubated at
424 30 °C (Y=4.9±3.6; r=0.100±0.030), suggesting that higher temperature tends to shift
425 *Methylobacterium* toward faster growth but lower efficiency, a typical trade-off observed in other
426 bacteria (51). The effect of monitoring temperature on growth rate was also independent from
427 time of sampling (no significant interaction in the ANOVA), suggesting that *Methylobacterium*
428 also grow faster and less efficiently at 30 °C regardless temporal environmental variations.
429 Accordingly, the pre-conditioning temperature had no effect on growth rate (p>0.05; ANOVA),
430 and very limited on yield (1.4%; p<0.05; ANOVA), suggesting limited effect of short-time
431 temperature shift on *Methylobacterium* growth performance (**Table 3**).
432
433 **Discussion**
434
435 *Methylobacterium* is ubiquitous on leaves in the temperate forests of Québec and its diversity in
436 this habitat is quite similar to what has been described in the phyllosphere throughout the world,
437 with three main clades A9 (*M. brachiatum*, *M. pseudosasicola*), A6 (*M. sp.*) and A1 (*M.*
438 *gossipicola*) dominating diversity in the canopy. Our barcoding approach based on a clade-
439 specific *rpoB* marker revealed astonishing diversity within these clades, as well as within several
440 other clades: B (*M. extorquens*), A2 (*M. sp.*), A4 (*M. gnaphalii*, *M. brachytecii*) and A10 (*M.*
441 *komagatae*) whose importance in the phyllosphere has been underestimated by classical 16S
442 barcoding or isolation approaches. This diversity, like that of the overall phyllosphere
443 community, was mostly determined by differences between forests, with barcoding approaches
444 suggesting combined effects of restricted migration, local adaptation to host tree species, and
445 climatic conditions at large geographical scales (>100km). With higher molecular resolution, we
446 observed that *Methylobacterium* diversity was structured even at the scale of a forest (within 2

447 km), which according to a fine-scale timeline survey over the growing season also showed a clear
448 pattern of temporal dynamics and succesion. A finer analysis of *Methylobacterium* diversity
449 suggested that clade identity partly explained *Methylobacterium* geographical distribution at large
450 scale (forest) but not at finer scales (plots), nor was it an indicator of adaptation to a particular
451 host tree species, nor a determinant of temporal dynamics. Rather, the distribution of
452 *Methylobacterium* diversity at small temporal and geographical scales likely resulted from more
453 contemporaneous community assembly events selecting for phenotypic traits that evolved among
454 deeply diverging lineages of *Methylobacterium*, as has been observed in other bacterial (16) and
455 plant clades (53).
456
457 We explored mechanisms explaining the temporal dynamics of *Methylobacterium* diversity at the
458 scale of a growing season. Because we observed contrasting *Methylobacterium* isolable diversity
459 between 20 and 30 °C, we suspected that adaptation to temperature variation during the growing
460 season could explain part of these temporal dynamics. By monitoring *Methylobacterium* isolate
461 growth under different temperature treatments, we confirmed that temperature affected isolate
462 growth performances. The fact that most tested isolates grow slower but more efficiently at 20 °C
463 than at 30 °C (**Figure 5d**), regardless of their phylogenetic and environmental characteristics, is
464 in line with a temperature-dependent trade-off between growth rate and yield described in many
465 bacteria (reviewed in (51)). High yield strategies are typical of cooperative bacterial populations,
466 while fast growth-strategies are typical of competitive populations (51), suggesting that 20 °C is
467 likely closer to the thermal niche of a cooperative *Methylobacterium* community, in agreement
468 with average temperatures in temperate forests during the growing season. This observation also
469 stresses the importance of considering incubation temperature when interpreting results from
470 previous studies assessing *Methylobacterium* diversity based on isolation. We observed several
471 lines of evidence that factors other than direct adaptation to temperature drive *Methylobacterium*
472 responses to temperature variation, by affecting their growth strategy in different competitive
473 conditions rather than by affecting their metabolism directly. First, clade identity was one of the
474 main predictors of overall isolate performance, with some clades (A1, A2, B) possessing a rapid
475 growth strategy under all temperature conditions, while others (clades A6, A9, A10) had
476 systematically slower growth. These clade-specific growth strategies could explain for instance
477 why certain *Methylobacterium* isolates are less competitive and less frequently isolated at higher

478 temperatures. Still, we cannot rule out that clade-specific growth strategy also reflect
479 experimental conditions. Second, we observed strong associations between isolates growth
480 performance and time of sampling, regardless of clade association, suggesting that growth
481 dynamic strategies also respond to seasonal variations in environmental conditions, and to the
482 level of establishment and competition in the phyllosphere community (51). This observation,
483 together with clade identity, could explain why, assuming that environmental conditions at the
484 end of the growing season became unfavorable for most strains, isolates from clades A1 and B
485 with a fast-growth strategy consistently increase in frequency during this period and lead to the
486 homogeneization of the community. Taken together, our temporal survey of diversity dynamics
487 and screening for growth performance suggest the following timeline of the dynamics of the
488 *Methylobacterium* phyllosphere community. At the very beginning of the growing season, a pool
489 of bacteria with mixed ecological strategies and genotypes colonizes newly emerging leaves. Due
490 to the stochasticity of this colonization, we initially observe strong dissimilarity among
491 phyllosphere communities, regardless of their spatial position. During the summer, optimal
492 environmental conditions allow the progressive establishment of a cooperative and structured
493 bacterial community with a high yield strategy (51). At the end of the growing season, with
494 migration, environmental conditions shifting and leaves senescing, isolates with a fast-growth
495 strategy are able to grow rapidly, dominating the phyllosphere community and leading to its
496 homogeneization before leaves fully senesce.
497
498 Our study illustrates that *Methylobacterium* is a complex group of divergent lineages with
499 different ecological strategies and distributions, reflecting long-term adaptation to highly
500 contrasted environments. Based upon a similar observation, some authors recently proposed to
501 reclassify *Methylobacterium* group B within a new genus (*Methylorubrum*) that they argue is
502 ecologically and evolutionarily distinct from other *Methylobacterium* clades (30). Although clade
503 B was well supported as a distinct clade in our analyses, our results suggest that it is in fact
504 embedded within clade A, which would render the genus *Methylobacterium* paraphyletic if clade
505 B is defined as a distinct genus (**Figure S5**), and group B was not particularly ecologically
506 distinct in comparison with other major clades (**Figure 1**). Our results emphasize the fact that
507 torough genomic investigations are needed to clarify the taxomonic status of *Methylobacterium*.
508 Beyond any taxonomic considerations, neither clade identity assessed by individual genetic

markers nor the tremendous ecological diversity among *Methylobacterium* clades can predict all of the spatial and temporal variation in *Methylobacterium* diversity in nature. In order to define the niches of *Methylobacterium* clades and to understand the metabolic mechanisms underlying their contrasted life strategies, future characterization of their functions and genome structure will be required using phylogenomic approaches.

In conclusion, we find that *Methylobacterium* adaptive responses to local environmental variation in the phyllosphere are driven by both long-term inherited ecological strategies that differ among major clades within the genus, as well by seasonal changes affecting habitat characteristics and community structure in the phyllosphere habitat. Overall, our study combining sequencing- and culture-based approaches provides novel insights into the factors driving fine-scale adaptation of microbes to their habitats, and in the case of *Methylobacterium* our approach revealed the particular importance of considering organismal life-history strategies to help understand the small-scale diversity and dynamic of this ecologically important taxon.

Figures and Table

Figure 1 - ***Methylobacterium*** **phylogeny and ecology.** Most of *Methylobacterium* diversity is found in association with plants, especially in the phyllosphere. Phylogenetic consensus tree (nodal posterior probabilities indicated next to the branches) from *rpoB* complete nucleotide sequences available for 153 *Methylobacterium* genomes and rooted on 32 *Methylobacteriaceae* outgroups (*Microvirga*, *Enterovirga*; no shown; see **Supplementary dataset 1a**). For each genome, species name, the anthropogenic origin (black squares) and/or environmental origin (color code on top right) are indicated. Groups A, B, C adapted from Green *et* Ardley (30). Monophyletic clades within group A (A1-A9) were defined using a 92% nucleotide pairwise similarity cut-off on the *rpoB* complete sequence.

Figure 2 - Sampling design. a) Locations of the two sampled forests MSH (green) and SBL (orange) in the province of Québec (Canada). b) Time line survey in each forest in 2018 (2-4 time points available per tree). c-d). Detailed map of each forest and each plot within forests (squares; 6 to 10 trees were sampled per plot; see **Supplementary dataset 1b**). In MSH, plots H0 and L0 were sampled once in 2017 for a pilot survey. In SBL and MSH, plots 1-6 were sampled 4 times in 2018. For each plot, tree localizations are indicated by point colored according to their taxonomie (color code on bottom left): ABBA (*Abies balsamea*), ACRU (*Acer rubrum*). ACSA (*Acer saccharum*), OSVI (*Ostrya virginiana*), QURU (*Quercus rubra*), FAGR (*Fagus grandifolia*), ASPE (*Acer Pennsylvanicum*). Shades of grey indicate elevation (50 m elevation scale)

Figure 3 - Tests for phylogenetic association of traits with culture-based estimation of *Methylobacterium* diversity. a) Part of variance in *Methylobacterium* isolated diversity explained by each trait and their interactions (PERMANOVA tests for association; 10,000 permutations; x-axis) in function of pairwise nucleotide similarity as a proxy for phylogenetic depth (PS; y-axis; see **Supplementary dataset 1i**). PERMANOVA were conducted at different depths within a consensus phylogenetic tree (nodes with less than 30% of support were collapsed; legend on top right) drawn from partial *rpoB* nucleotide sequences of 187 isolates (pilot survey in 2017: n=20; timeline survey in 2018: n=167) and 188 *Methylobacteriaceae* reference sequences.

The four following traits and their interactions were tested (see Venn diagram on top left for color code): forest of origin, host tree species, sampling date and temperature of isolation. Points indicate significant part of variance (legend on the left). b) Test for node association (100,000 permutations) with forest of origin and temperature of isolation (color code on top) mapped on the *rpoB* phylogeny (scaled on PS values). Frames in the tree indicate nodes significantly associated with at least one factor (ANOVA; Bonferroni correction; $p<0.001$: "***"; $p<0.01$:"**"; $p<0.05$:"*"). For each isolate (names in bold), colored boxes at the tip of the tree indicate forest of origin and temperature of isolation.

Figure 4 - Short-scale spatial and temporal dynamics of *Methylobacterium* communities assessed by *rpoB* barcoding. a) A principal component analysis (PCA) on 200 *Methylobacterium* ASVs relative abundance (Hellinger transformation, Bray-Curtis (*BC*) dissimilarity) shows that 179 phyllosphere samples cluster according to forest of origin (MSH: open triangles, SBL: full triangles) and date of sampling (detail showed only for MSH). The significant association of 83 and 25 ASVs with forest of origin and/or sampling date, respectively (ANOVA, Bonferroni correction; $p<0.05$; point size proportional to variance; legend on bottom left) is shown (points colored according to clade assignation; legend on top right). b) Spatial and c) temporal autocorrelation analyzes conducted in each forest separately. Points represent BC dissimilarity in function of pairwise geographic (*pDist*; b) or pairwise time (*pTime*; c) distance separating two communities. For each forest and variable, the predicted linear regression (*BC~pDIST* or *~pTime*) is indicated (full line: $p<0.001$; dotted line: $p>0.05$; ANOVA). d) *BC* in function of sampling time for each forest. e) Detail of spatial autocorrelation analyzes in MSH, conducted for each sampling time point separately. f) Scaled ML tree (original tree from **Figure S1b** scaled on pairwise nucleotide similarity (PS)) of 200 *Methylobacterium* ASV (points) and 176 reference *rpoB* sequences rooted on *Microvirga* and *Enterovirga* (out group not shown). Temporal autocorrelation analyzes per forest were conducted for each node supported by at least 30% of bootstraps (200 permutations). For each forest and node, the strength of the slope (estimate of the linear regression *BC~pTime*; proportional to point size) was displayed when highly significant ($p<0.001$; ANOVA, Bonferroni correction).

588 **Figure 5 - Analysis of 79 *Methylobacterium* isolate growth performances under 4 different**
589 **temperature treatments.** For each isolate and temperature treatment, the yield (*Y*: maximal
590 growth intensity) and growth rate (*r*; inverse of log+lag time) were estimated from growth
591 curves. a) Average growth curves (growth intensity in function of time) for each clade (line:
592 mean value; frame: 1/3 of standard deviation; point: average maximal growth). b) *r* in function of
593 *Y*. Each point represents the average *r*/*Y* values for an isolate and a temperature treatment (79
594 isolates x 4 treatments), colored according to clade membership. Ellipsoides are centered on
595 average values per clade and represent 30% of confidence interval (standard deviation). c) *r* (log
596 scale) in function of time at which samples strains were isolated from were collected, colored
597 according to the forest of origin. Points: real data; bars: average *r* value per forest (n=2) and time
598 (n=4) category. d) *r* in function of Y, corrected for clade assignement (residuals of the *r*~Clade
599 and *Y*~Clade linear regressions). Each point represents the average *r*/*Y* residual values for an
600 isolate and a temperature treatment (79 isolates x 4 treatments), colored according to monitoring
601 temperature (legend on top right).
602
603

Table 1 - PERMANOVA analysis of variance in *Bacteria* and *Methylobacterium* community diversity. *Bacteria* diversity was assessed by *16s* barcoding in 46 phyllosphere samples. *Methylobacterium* was assessed by *rpoB* barcoding after filtering out non-*Methylobacterium* diversity in 179 phyllopshere samples. Part of variance in dissimilarity (R^2; Bray-Curtis index) among samples associated with four factors and their possible interactions (*F*: forest of origin; *D*: date of sampling; *H*: host tree species; *P*: plot within forest) and their significance are shown (10,000 permutations on ASV relative abundance, Hellinger transformation; "***": p<0.00l; "**": p<0.01; "*": p<0.05.) For 16s, *P* was omitted to conserve degrees of freedom.

	***Bacteria* (*16s*)**		***Methylobacterium (rpoB)***	
Samples	**46**		**179**	
Factor	**R^2**	**Pr(>F)**	**R^2**	**Pr(>F)**
Forest of origin (F)	0.316***	<0.000	0.324***	<0.001
Host tree specie (H)	0.156***	<0.001	0.071***	<0.001
Time of sampling (D)	0.120*	0.016	0.048***	<0.001
Plot within forests (P)	-	-	0.080***	<0.001
F:H	0.020	0.080	0.004	0.110
H:D	0.239	0.217	0.074**	0.028
H:P	-	-	0.043**	0.007
D:P	-	-	0.058	0.455
H:D:P	-	-	0.085	0.052
Residuals	0.150	-	0.213	-

Table 2 - Summary of statistics from autocorrelation analyzes on 179 phyllosphere *Methylobacterium* samples assessed by *rpoB* barcoding (200 ASVs). For each model, pairwise dissimilarity between two communities was assessed with the Bray-Curtis dissimilarity index (*BC*) from ASV relative abundance (Hellinger transformation) under a linear model. *Spatial autocorrelation general models* : *BC* in function of pairwise spatial distance separating two sampled trees (*pDist*) and date of sampling (*Date*) and their interaction (*pDist:Date*). Samples from forests MSH and SBL were analyzed separately (two models). Only pairwise comparisons among samples from a same date were considered. *Spatial autocorrelation models per date*: *BC* in function of pairwise spatial distance (*pDist*). Each sampling date (n=4) and forest (n=2) was analyzed separately (eight models). *Temporal autocorrelation: general models*: *BC* in function of pairwise spatial time separating two sampled trees (*pTime*). Samples from forests MSH and SBL were analyzed separately (two models) and all spatial scales were considered. For each model, the average and standard deviation of the intercept (mean BC value) are indicated. For each factor (*pDist*, *Date*, *pDist:Date* and *pTime*), the average and standard deviation of estimates (slope) are indicated. Significance of estimates was assessed by ANOVA ("***": p<0.00l; "**": p<0.01; "*": p<0.05).

Categories (*n*)	**Intercept (sd)**		**Estimates*10^{-3} (sd)**	
*Spatial autocorrelation general models: lm(BC ~pDist*D)*				
Site (within dates)	*BC*	*pDist*	*D*	*pDist:Date*
MSH	0.5965 (0.0107)	**-0.0041 (0.0192)*** **	**-2.7648 (0.1313)*** **	**0.0007 (0.0002)** **
SBL	0.6493 (0.0097)	0.0157 (0.0145)	**-1.5575 (0.1646)*** **	0.0000 (0.0002)
Spatial autocorrelation models per date: lm(BC ~pDist)				
Site	**Date**	*BC*	*pDist*	
MSH	**27 Jun.**	0.6237 (0.0340)	-0.0425 (0.0725)	
	6 Aug.	0.4919 (0.0112)	**0.0503 (0.0192)** **	
	7 Sept.	0.3746 (0.0059)	**0.0313 (0.0099)** **	
	18 Oct.	0.2966 (0.0045)	**0.0795 (0.0073)*** **	
SBL	**20 Jun.**	0.6868 (0.0146)	0.0082 (0.0216)	
	16 Jul.	0.5819 (0.0113)	0.0215 (0.0174)	
	16 Aug.	0.5415 (0.0105)	0.0114 (0.0150)	
	20 Sept.	0.5222 (0.0089)	0.0145 (0.0130)	
Temporal autocorrelation general models (BC ~pTime)				
Site		*BC*	*pTime*	
MSH		0.4086 (0.0032)	**1.0786 (0.0607)*** **	
SBL		0.5789 (0.0030)	**0.3012 (0.0617)*** **	

Table 3 - Part of variance in yield (*Y*) and growth rate (*r*) measured in 79 *Methylobacterium* isolates grown under 4 temperature treatments. *Y* and *r* values were transformed in log to meet normal distribution. Significance of *Y* and *r* response were evaluated by ANOVA in linear models: $\log(Y) \sim F*H*D*T_p*T_M*C$ *and* $\log(r) \sim F*H*D*T_p*T_M*C$, respectively, with following factors : clade (*C*), forest of origin (*F*), host tree species (*H*), time of sampling (*D*), temperature of incubation during pre-conditioning (T_P) and monitoring (T_M) steps and their interactions (only significant are shown: "***": p<0.00l; "**": p<0.01; "*": p<0.05).

	Rate	Yield
Forest (*F*)	0.015*	0.002
Host tree species (*H*)	0.022**	0.013**
Date of sampling (*D*)	0.054***	0.013**
Pre-conditioning temperature (*TP*)	0.001	0.014**
Monitoring temperature (*TM*)	0.158***	0.020**
Clade (*C*)	0.076***	0.306***
F:D	0.006	0.036***
H:D	0.001	0.015**
H:C	0.006	0.058***
D:C	0.032*	0.022*
F:H:D	0.019**	0.035***
F:H:C	0.013*	0.006
other interactions	0.142	0.084
Residuals	0.456	0.377

References

1. Vorholt JA. 2012. Microbial life in the phyllosphere. 12. Nature Reviews Microbiology 10:828–840.

2. Lindow SE, Brandl MT. 2003. Microbiology of the Phyllosphere. Appl Environ Microbiol 69:1875–1883.

3. Fürnkranz M, Wanek W, Richter A, Abell G, Rasche F, Sessitsch A. 2008. Nitrogen fixation by phyllosphere bacteria associated with higher plants and their colonizing epiphytes of a tropical lowland rainforest of Costa Rica. 5. The ISME Journal 2:561–570.

4. Laforest-Lapointe I, Messier C, Kembel SW. 2016. Host species identity, site and time drive temperate tree phyllosphere bacterial community structure. Microbiome 4:27.

5. Laforest-Lapointe I, Messier C, Kembel SW. 2016. Tree phyllosphere bacterial communities: exploring the magnitude of intra- and inter-individual variation among host species. PeerJ 4:e2367.

6. Noble AS, Noe S, Clearwater MJ, Lee CK. 2020. A core phyllosphere microbiome exists across distant populations of a tree species indigenous to New Zealand. PLOS ONE 15:e0237079.

7. Kembel SW, O'Connor TK, Arnold HK, Hubbell SP, Wright SJ, Green JL. 2014. Relationships between phyllosphere bacterial communities and plant functional traits in a neotropical forest. PNAS 111:13715–13720.

8. Shade A, Gregory Caporaso J, Handelsman J, Knight R, Fierer N. 2013. A meta-analysis of changes in bacterial and archaeal communities with time. 8. The ISME Journal 7:1493–1506.

9. Malik AA, Martiny JBH, Brodie EL, Martiny AC, Treseder KK, Allison SD. 2020. Defining trait-based microbial strategies with consequences for soil carbon cycling under climate change. 1. The ISME Journal 14:1–9.

10. Moyes AB, Kueppers LM, Pett□Ridge J, Carper DL, Vandehey N, O'Neil J, Frank AC. 2016. Evidence for foliar endophytic nitrogen fixation in a widely distributed subalpine conifer. New Phytologist 210:657–668.

11. Lajoie G, Kembel SW. 2019. Making the Most of Trait-Based Approaches for Microbial Ecology. Trends in Microbiology 27:814–823.

12. Nemergut DR, Schmidt SK, Fukami T, O'Neill SP, Bilinski TM, Stanish LF, Knelman JE, Darcy JL, Lynch RC, Wickey P, Ferrenberg S. 2013. Patterns and Processes of Microbial

673 Community Assembly. Microbiol Mol Biol Rev 77:342–356.
674 13. Cavender□Bares J, Kozak KH, Fine PVA, Kembel SW. 2009. The merging of
675 community ecology and phylogenetic biology. Ecology Letters 12:693–715.
676 14. Martiny JBH, Jones SE, Lennon JT, Martiny AC. 2015. Microbiomes in light of traits: A
677 phylogenetic perspective. Science 350.
678 15. Tromas N, Taranu ZE, Castelli M, Pimentel JSM, Pereira DA, Marcoz R, Shapiro BJ,
679 Giani A. 2020. The evolution of realized niches within freshwater Synechococcus.
680 Environmental Microbiology 22:1238–1250.
681 16. Tromas N, Taranu ZE, Martin BD, Willis A, Fortin N, Greer CW, Shapiro BJ. 2018.
682 Niche Separation Increases With Genetic Distance Among Bloom-Forming Cyanobacteria. Front
683 Microbiol 9.
684 17. Thompson LR, Sanders JG, McDonald D, Amir A, Ladau J, Locey KJ, Prill RJ, Tripathi
685 A, Gibbons SM, Ackermann G, Navas-Molina JA, Janssen S, Kopylova E, Vázquez-Baeza Y,
686 González A, Morton JT, Mirarab S, Zech Xu Z, Jiang L, Haroon MF, Kanbar J, Zhu Q, Jin Song
687 S, Kosciolek T, Bokulich NA, Lefler J, Brislawn CJ, Humphrey G, Owens SM, Hampton-
688 Marcell J, Berg-Lyons D, McKenzie V, Fierer N, Fuhrman JA, Clauset A, Stevens RL, Shade A,
689 Pollard KS, Goodwin KD, Jansson JK, Gilbert JA, Knight R. 2017. A communal catalogue
690 reveals Earth's multiscale microbial diversity. 7681. Nature 551:457–463.
691 18. Poretsky R, Rodriguez-R LM, Luo C, Tsementzi D, Konstantinidis KT. 2014. Strengths
692 and Limitations of 16S rRNA Gene Amplicon Sequencing in Revealing Temporal Microbial
693 Community Dynamics. PLOS ONE 9:e93827.
694 19. Ranjan R, Rani A, Metwally A, McGee HS, Perkins DL. 2016. Analysis of the
695 microbiome: Advantages of whole genome shotgun versus 16S amplicon sequencing.
696 Biochemical and Biophysical Research Communications 469:967–977.
697 20. Corpe WA, Rheem S. 1989. Ecology of the methylotrophic bacteria on living leaf
698 surfaces. FEMS Microbiol Ecol 5:243–249.
699 21. Keppler F, Hamilton JTG, Braß M, Röckmann T. 2006. Methane emissions from
700 terrestrial plants under aerobic conditions. 7073. Nature 439:187–191.
701 22. Clarke PH. 1983. The biochemistry of Methylotrophs by C. Anthony Academic Press;
702 London, New York, 1982 xvi + 432 pages. £24.00, $49.50. FEBS Letters 160:303–303.
703 23. Anthony C. 1991. Assimilation of carbon by methylotrophs. Biotechnology 18:79–109.

704 24. Ivanova EG, Doronina NV, Trotsenko YuA. 2001. Aerobic Methylobacteria Are Capable
705 of Synthesizing Auxins. Microbiology 70:392–397.
706 25. Madhaiyan M, Poonguzhali S, Lee HS, Hari K, Sundaram SP, Sa TM. 2005. Pink-
707 pigmented facultative methylotrophic bacteria accelerate germination, growth and yield of
708 sugarcane clone Co86032 (Saccharum officinarum L.). Biol Fertil Soils 41:350–358.
709 26. Madhaiyan M, Poonguzhali S, Sa T. 2007. Metal tolerating methylotrophic bacteria
710 reduces nickel and cadmium toxicity and promotes plant growth of tomato (Lycopersicon
711 esculentum L.). Chemosphere 69:220–228.
712 27. Dourado MN, Aparecida Camargo Neves A, Santos DS, Araújo WL. 2015.
713 Biotechnological and Agronomic Potential of Endophytic Pink-Pigmented Methylotrophic
714 Methylobacterium spp. Biomed Res Int 2015.
715 28. Ryu JH (Chungbuk NU, Madhaiyan M (Chungbuk NU, Poonguzhali S (Chungbuk NU,
716 Yim WJ (Chungbuk NU, Indiragandhi P (Chungbuk NU, Kim KA (Chungbuk NU, Anandham R
717 (Chungbuk NU, Yun JC (National I of AS and T, Kim KH (The U of S, Sa TM (Chungbuk NU.
718 2006. Plant Growth Substances Produced by Methylobacterium spp. and Their Effect on Tomato
719 (Lycopersicon esculentum L.) and Red Pepper (Capsicum annuum L.) Growth. Journal of
720 Microbiology and Biotechnology.
721 29. Lee HS, Madhaiyan M, Kim CW, Choi SJ, Chung KY, Sa TM. 2006. Physiological
722 enhancement of early growth of rice seedlings (Oryza sativa L.) by production of phytohormone
723 of N2-fixing methylotrophic isolates. Biol Fertil Soils 42:402–408.
724 30. Green PN, Ardley JK. 2018. Review of the genus Methylobacterium and closely related
725 organisms: a proposal that some Methylobacterium species be reclassified into a new genus,
726 Methylorubrum gen. nov. International Journal of Systematic and Evolutionary Microbiology
727 68:2727–2748.
728 31. Chen W-M, Cai C-Y, Li Z-H, Young C-C, Sheu S-Y. 2019. Methylobacterium
729 oryzihabitans sp. nov., isolated from water sampled from a rice paddy field. International Journal
730 of Systematic and Evolutionary Microbiology, 69:3843–3850.
731 32. Feng G-D, Chen W, Zhang X-J, Zhang J, Wang S-N, Zhu H. 2020. Methylobacterium
732 nonmethylotrophicum sp. nov., isolated from tungsten mine tailing. International Journal of
733 Systematic and Evolutionary Microbiology, 70:2867–2872.
734 33. Jia L juan, Zhang K shuai, Tang K, Meng J yu, Zheng C, Feng F ying. 2020.

735 Methylobacterium crusticola sp. nov., isolated from biological soil crusts. International Journal of
736 Systematic and Evolutionary Microbiology, 70:2089–2095.
737 34. Kim J, Chhetri G, Kim I, Lee B, Jang W, Kim MK, Seo T. 2020. Methylobacterium
738 terricola sp. nov., a gamma radiation-resistant bacterium isolated from gamma ray-irradiated soil.
739 International Journal of Systematic and Evolutionary Microbiology, 70:2449–2456.
740 35. Kim J, Chhetri G, Kim I, Kim MK, Seo T. 2020. Methylobacterium durans sp. nov., a
741 radiation-resistant bacterium isolated from gamma ray-irradiated soil. Antonie van Leeuwenhoek
742 113:211–220.
743 36. Ten LN, Li W, Elderiny NS, Kim MK, Lee S-Y, Rooney AP, Jung H-Y. 2020.
744 Methylobacterium segetis sp. nov., a novel member of the family Methylobacteriaceae isolated
745 from soil on Jeju Island. Arch Microbiol 202:747–754.
746 37. Jiang L, An D, Wang X, Zhang K, Li G, Lang L, Wang L, Jiang C, Jiang Y. 2020.
747 Methylobacterium planium sp. nov., isolated from a lichen sample. Arch Microbiol 202:1709–
748 1715.
749 38. Pascual JA, Ros M, Martínez J, Carmona F, Bernabé A, Torres R, Lucena T, Aznar R,
750 Arahal DR, Fernández F. 2020. Methylobacterium symbioticum sp. nov., a new species isolated
751 from spores of Glomus iranicum var. tenuihypharum. Curr Microbiol 77:2031–2041.
752 39. Marx CJ, Bringel F, Chistoserdova L, Moulin L, Farhan Ul Haque M, Fleischman DE,
753 Gruffaz C, Jourand P, Knief C, Lee M-C, Muller EEL, Nadalig T, Peyraud R, Roselli S, Russ L,
754 Goodwin LA, Ivanova N, Kyrpides N, Lajus A, Land ML, Médigue C, Mikhailova N, Nolan M,
755 Woyke T, Stolyar S, Vorholt JA, Vuilleumier S. 2012. Complete Genome Sequences of Six
756 Strains of the Genus Methylobacterium. J Bacteriol 194:4746–4748.
757 40. Tani A, Ogura Y, Hayashi T, Kimbara K. 2015. Complete Genome Sequence of
758 Methylobacterium aquaticum Strain 22A, Isolated from Racomitrium japonicum Moss. Genome
759 Announc 3.
760 41. Minami T, Ohtsubo Y, Anda M, Nagata Y, Tsuda M, Mitsui H, Sugawara M,
761 Minamisawa K. 2016. Complete Genome Sequence of Methylobacterium sp. Strain AMS5, an
762 Isolate from a Soybean Stem. Genome Announc 4.
763 42. Morohoshi T, Ikeda T. 2016. Complete Genome Sequence of Methylobacterium populi P-
764 1M, Isolated from Pink-Pigmented Household Biofilm. Genome Announc 4.
765 43. Belkhelfa S, Labadie K, Cruaud C, Aury J-M, Roche D, Bouzon M, Salanoubat M,

766 Döring V. 2018. Complete Genome Sequence of the Facultative Methylotroph Methylobacterium
767 extorquens TK 0001 Isolated from Soil in Poland. Genome Announc 6.
768 44. Vos M, Quince C, Pijl AS, Hollander M de, Kowalchuk GA. 2012. A Comparison of
769 rpoB and 16S rRNA as Markers in Pyrosequencing Studies of Bacterial Diversity. PLOS ONE
770 7:e30600.
771 45. Ogier J-C, Pagès S, Galan M, Barret M, Gaudriault S. 2019. rpoB, a promising marker for
772 analyzing the diversity of bacterial communities by amplicon sequencing. BMC Microbiol
773 19:171.
774 46. Callahan BJ, McMurdie PJ, Rosen MJ, Han AW, Johnson AJA, Holmes SP. 2016.
775 DADA2: High resolution sample inference from Illumina amplicon data. Nat Methods 13:581–
776 583.
777 47. Green PN. 2015. Methylobacterium, p. 1–8. *In* Bergey's Manual of Systematics of
778 Archaea and Bacteria. American Cancer Society.
779 48. Charron G, Leducq JB, Bertin C, Dube AK, Landry CR. 2014. Exploring the northern
780 limit of the distribution of Saccharomyces cerevisiae and Saccharomyces paradoxus in North
781 America. FEMS Yeast Res 14:281–8.
782 49. Leducq JB, Charron G, Samani P, Dube AK, Sylvester K, James B, Almeida P, Sampaio
783 JP, Hittinger CT, Bell G, Landry CR. 2014. Local climatic adaptation in a widespread
784 microorganism. Proceedings Biological sciences / The Royal Society 281:20132472.
785 50. Zwietering MH, Jongenburger I, Rombouts FM, Riet K van 't. 1990. Modeling of the
786 Bacterial Growth Curve. Appl Environ Microbiol 56:1875–1881.
787 51. Lipson DA. 2015. The complex relationship between microbial growth rate and yield and
788 its implications for ecosystem processes. Front Microbiol 6.
789 52. MacArthur RH, Wilson EO. 2001. The Theory of Island Biogeography. Princeton
790 University Press.
791 53. Cavender□Bares J, Ackerly DD, Baum DA, Bazzaz FA. 2004. Phylogenetic
792 Overdispersion in Floridian Oak Communities. The American Naturalist 163:823–843.
793

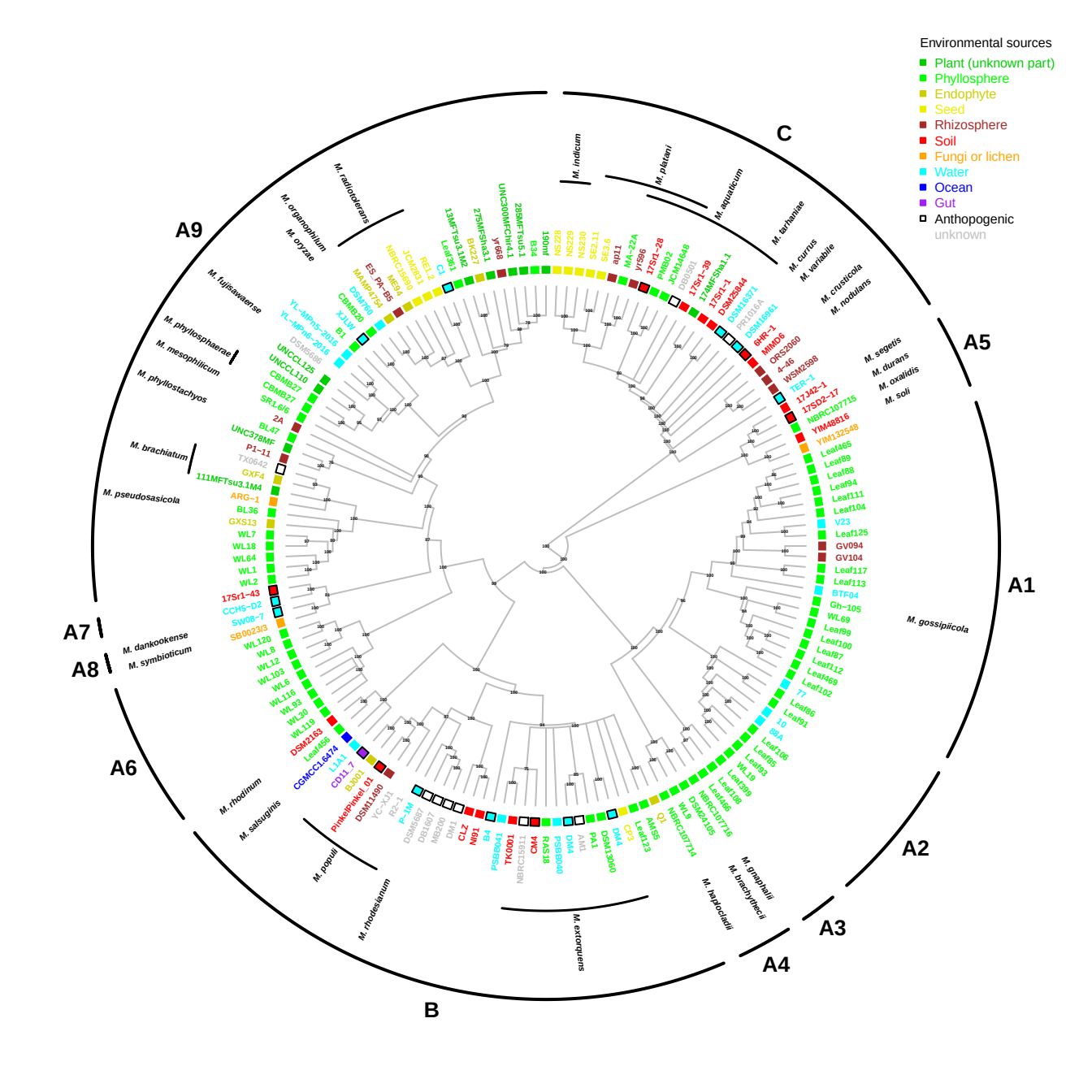
Environmental sources
Plant (unknown part)
Phyllosphere
Endophyte
Seed
Rhizosphere
Soil
Fungi or lichen
Water
Ocean
Gut
Anthopogenic
unknown
A1
A2
A3
A4
A5
A6
A7
A8
A9
B
C
M. indicum
M. platani
M. aquaticum
M. tarhanae
M. currus
M. variabile
M. crusticola
M. nodulans
M. segetis
M. durans
M. oxalidis
M. soli
M. gossipiicola
M. graphalii
M. brachythecii
M. hapalocladii
M. extorquens
M. rhodesianum
M. populi
M. salsuginis
M. rhodinum
M. dankookense
M. symbioticum
M. pseudosasicola
M. brachiatum
M. phyllostachyos
M. mesophilicum
M. phyllosphaerae
M. fujisawaense
M. oryzae
M. organophilum
M. radiotolerans

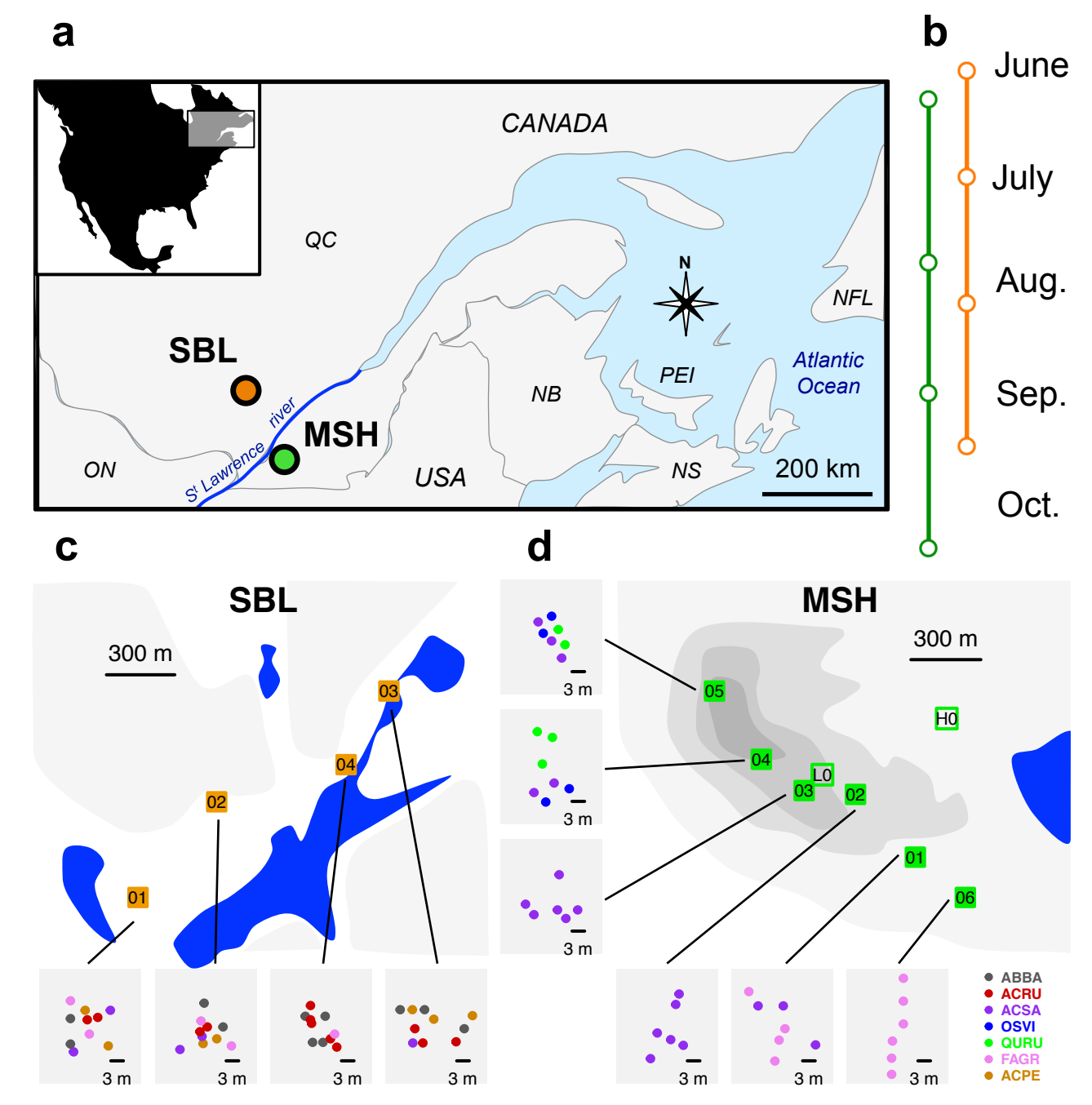
a
CANADA
QC
SBL
MSH
St Lawrence river
ON
USA
NB
PEI
NS
NFL
Atlantic Ocean
N
200 km
b
June
July
Aug.
Sep.
Oct.
c
SBL
300 m
01
02
03
04
3 m
d
MSH
300 m
05
04
03
02
01
06
H0
L0
3 m
ABBA
ACRU
ACSA
OSVI
QURU
FAGR
ACPE

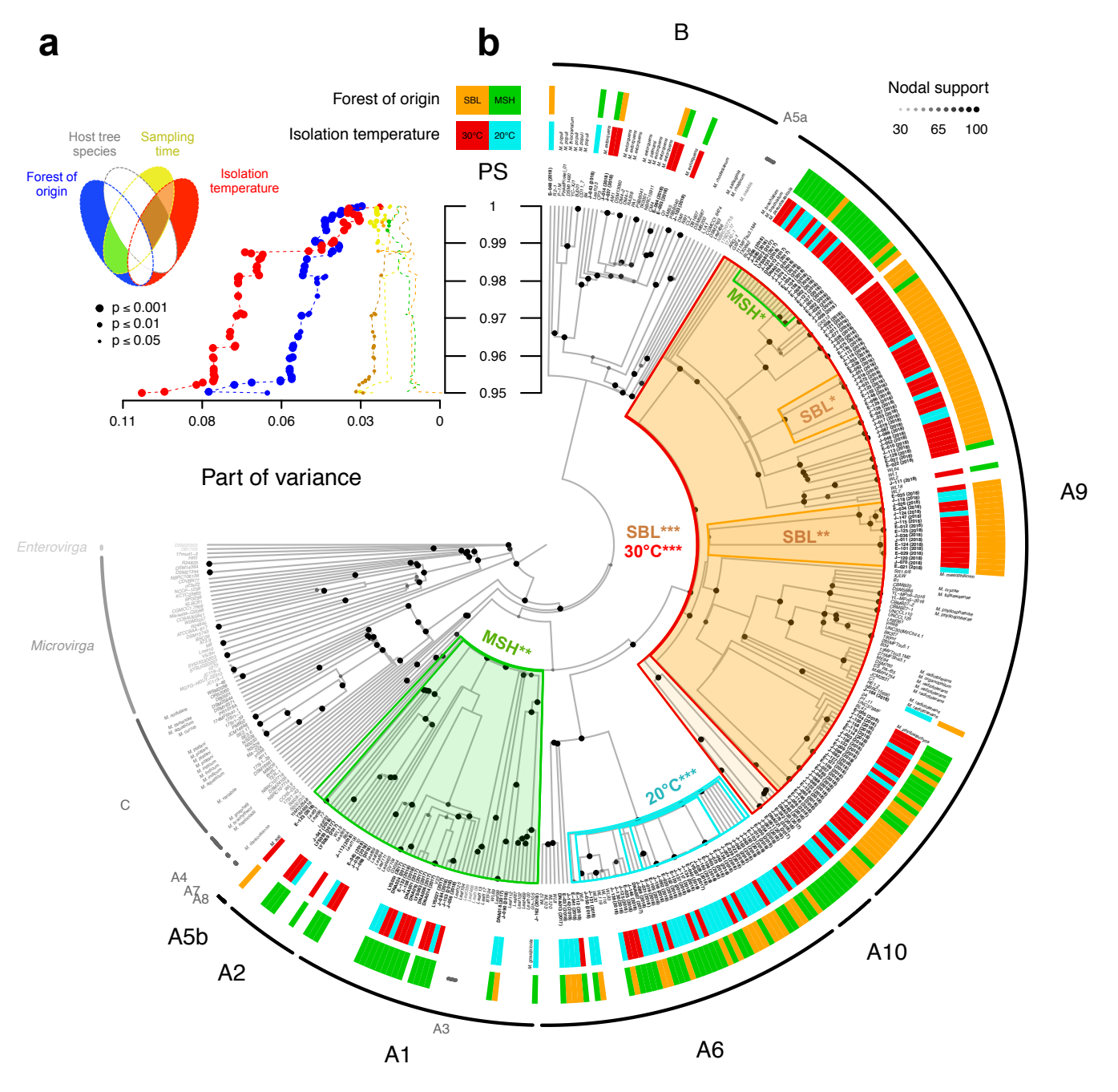
a
Host tree species
Sampling time
Forest of origin
Isolation temperature
p ≤ 0.001
p ≤ 0.01
p ≤ 0.05
0.11
0.08
0.06
0.03
0
Part of variance
b
Forest of origin
SBL
MSH
Isolation temperature
30°C
20°C
PS
1
0.99
0.98
0.97
0.96
0.95
Nodal support
30
65
100
B
A5a
A9
A10
A6
A1
A3
A2
A5b
A4
A7
A8
C
Enterovirga
Microvirga
MSH*
SBL*
SBL**
SBL***
30°C***
MSH**
20°C***

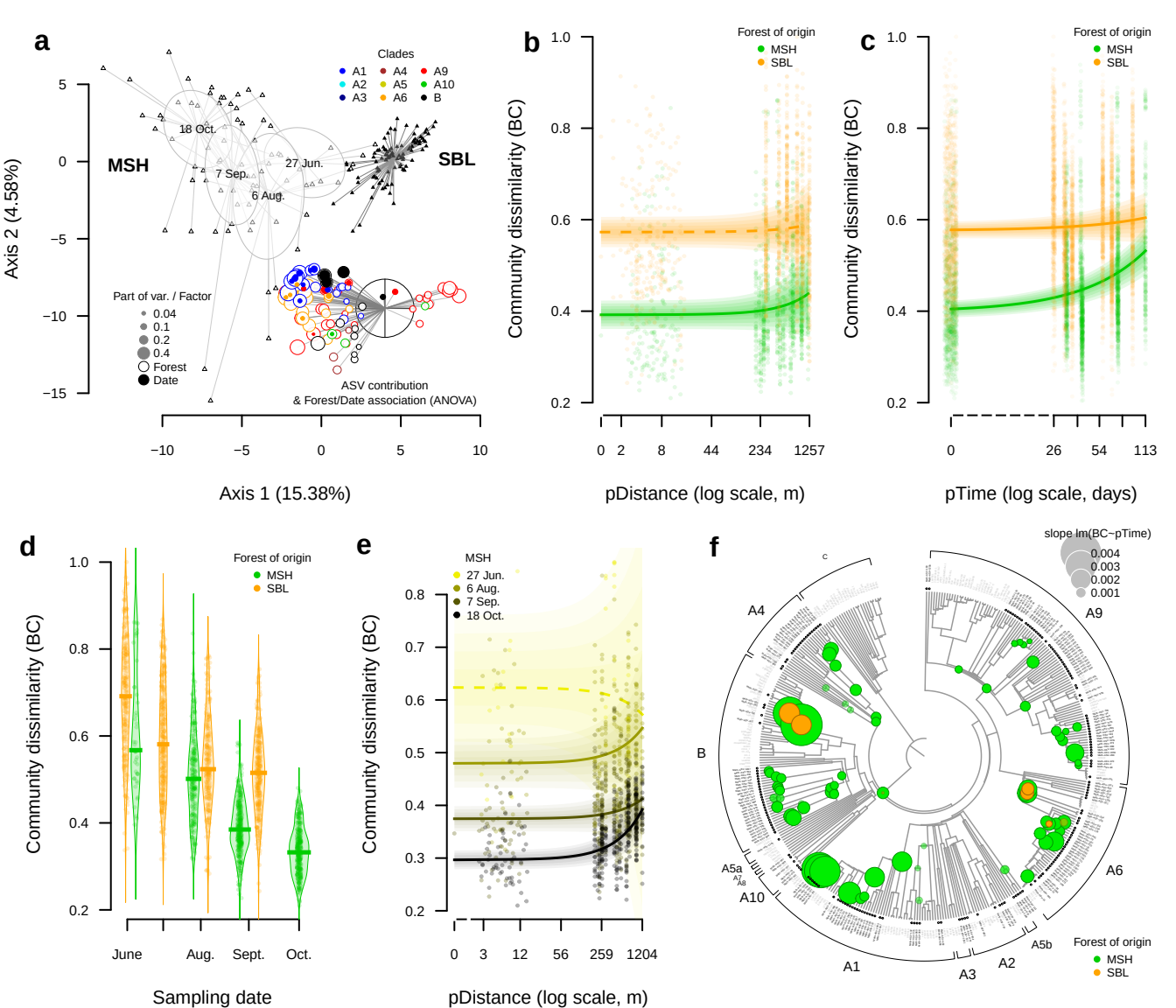
a
Clades
A1
A2
A3
A4
A5
A6
A9
A10
B
MSH
SBL
18 Oct.
7 Sep.
6 Aug.
27 Jun.
Part of var. / Factor
0.04
0.1
0.2
0.4
Forest
Date
ASV contribution
& Forest/Date association (ANOVA)
Axis 2 (4.58%)
Axis 1 (15.38%)
b
Forest of origin
MSH
SBL
Community dissimilarity (BC)
pDistance (log scale, m)
c
Forest of origin
MSH
SBL
Community dissimilarity (BC)
pTime (log scale, days)
d
Forest of origin
MSH
SBL
Community dissimilarity (BC)
June
Aug.
Sept.
Oct.
Sampling date
e
MSH
27 Jun.
6 Aug.
7 Sep.
18 Oct.
Community dissimilarity (BC)
pDistance (log scale, m)
f
slope lm(BC~pTime)
0.004
0.003
0.002
0.001
A4
A9
B
A6
A10
A1
A3
A2
A5b
Forest of origin
MSH
SBL

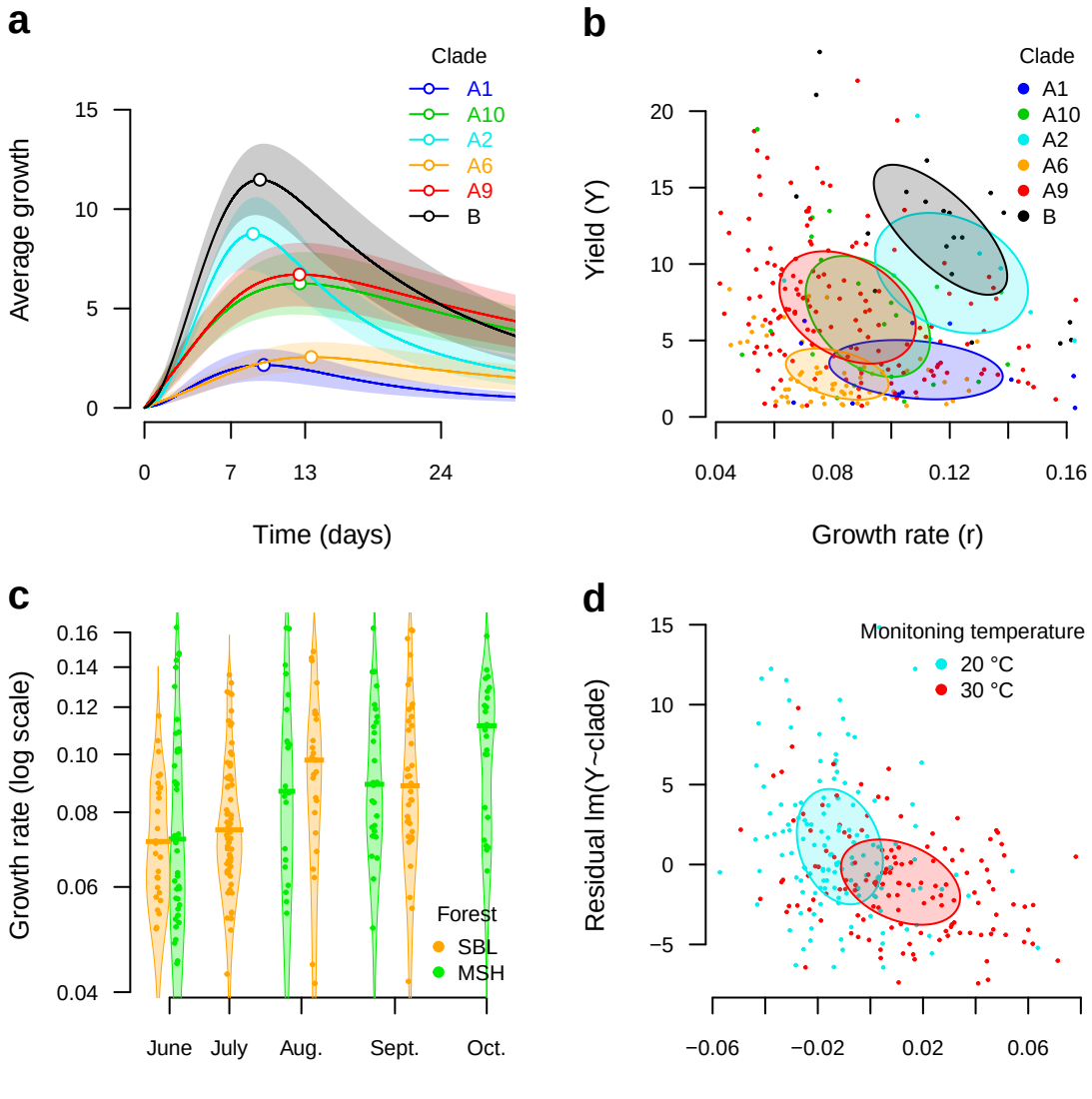
a
Clade
A1
A10
A2
A6
A9
B
Average growth
15
10
5
0
0
7
13
24
Time (days)
b
Clade
A1
A10
A2
A6
A9
B
Yield (Y)
20
15
10
5
0
0.04
0.08
0.12
0.16
Growth rate (r)
c
Growth rate (log scale)
0.16
0.14
0.12
0.10
0.08
0.06
0.04
Forest
SBL
MSH
June
July
Aug.
Sept.
Oct.
Sampling date
d
Monitoning temperature
20 °C
30 °C
Residual lm(Y~clade)
15
10
5
0
−5
−0.06
−0.02
0.02
0.06
Residual lm(r~clade)